Chemical Research in Toxicology

Article

Cite This: Chem. Res. Toxicol. 2018, 31, 48−57

pubs.acs.org/crt

Methyl DNA Phosphate Adduct Formation in Rats Treated Chronically with 4-(Methylnitrosamino)-1-(3-pyridyl)-1-butanone and Enantiomers of Its Metabolite 4-(Methylnitrosamino)-1-(3-pyridyl)-1-butanol

Bin Ma,* Adam T. Zarth, Erik S. Carlson, Peter W. Villalta, Pramod Upadhyaya, Irina Stepanov, and Stephen S. Hecht

Masonic Cancer Center, University of Minnesota, 2231 Sixth Street SE, 2-152 CCRB, Minneapolis, Minnesota 55455, United States

Supporting Information

ABSTRACT: The tobacco-specific nitrosamine 4-(methylnitrosamino)-1-(3-pyridyl)-1-butanone (NNK) is a powerful lung carcinogen in animal models and is considered a causative factor for lung cancer in tobacco users. NNK is stereoselectively and reversibly metabolized to 4-(methylnitrosamino)-1-(3-pyridyl)-1-butanol (NNAL), which is also a lung carcinogen. Both NNK and NNAL undergo metabolic activation by α-hydroxylation on their methyl groups to form pyridyloxobutyl and pyridylhydroxybutyl DNA base and phosphate adducts, respectively. α-Hydroxylation also occurs on the α-methylene carbons of NNK and NNAL to produce methane diazohydroxide, which reacts with DNA to form methyl DNA base adducts. DNA adducts of NNK and NNAL are important in their mechanisms of carcinogenesis. In this study, we characterized and quantified methyl DNA phosphate adducts in the lung of rats treated with 5 ppm of NNK, (*S*)-NNAL, or (*R*)-NNAL in drinking water for 10, 30, 50, and 70 weeks, by using a novel liquid chromatography-nanoelectrospray ionization-high resolution tandem mass spectrometry method. A total of 23, 21, and 22 out of 32 possible methyl DNA phosphate adducts were detected in the lung tissues of rats treated with NNK, (*S*)-NNAL, and (*R*)-NNAL, respectively. Levels of the methyl DNA phosphate adducts were 2290−4510, 872−1120, and 763−1430 fmol/mg DNA, accounting for 15−38%, 8%, and 5−9% of the total measured DNA adducts in rats treated with NNK, (*S*)-NNAL, and (*R*)-NNAL, respectively. The methyl DNA phosphate adducts characterized in this study further enriched the diversity of DNA adducts formed by NNK and NNAL. These results provide important new data regarding NNK- and NNAL-derived DNA damage and new insights pertinent to future mechanistic and biomonitoring studies of NNK, NNAL, and other chemical methylating agents.

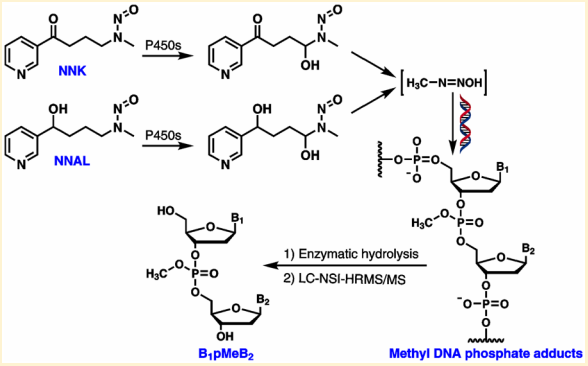

INTRODUCTION

The tobacco-specific nitrosamine 4-(methylnitrosamino)-1-(3-pyridyl)-1-butanone (NNK, **1**, Figure 1) is a potent lung carcinogen in animal models[1] and, together with the related compound *N*′-nitrosonornicotine, is classified as a human carcinogen (Group 1) by the International Agency for Research on Cancer.[2] NNK is metabolized to 4-(methylnitrosamino)-1-(3-pyridyl)-1-butanol (NNAL, **2**, Figure 1), which is also a potent lung carcinogen with activity similar to NNK.[1,3,4] Both NNK and NNAL are metabolically activated by α-hydroxylation catalyzed by cytochrome P450s to form a series of intermediates which react with DNA to form adducts. The formation of these DNA adducts can cause miscoding and mutations in growth control genes,[5−7] which is a critical step in carcinogenesis by NNK and NNAL. Therefore, identification and measurement of relevant DNA adducts can enhance our understanding of mechanisms of NNK- and NNAL-associated carcinogenesis and tobacco-related cancers.

Metabolic activation of NNK by α-hydroxylation on its methyl group produces an unstable intermediate α-hydroxymethylNNK (**3**) which decomposes to 4-(3-pyridyl)-4-oxobutane-1-diazohydroxide (**7**) that reacts with DNA to form adducts (Figure 1). These adducts are formed by alkylation of nucleobases to produce pyridyloxobutyl (POB) base adducts[8,9] and by alkylation of the oxygen of the internucleoside phosphodiester linkages in the DNA to produce pyridyloxobutyl phosphate adducts [B_1p(POB)B_2],[10] where B_1 and B_2 represent the same or different nucleobases. Similar to NNK, α-hydroxylation on the methyl group of NNAL produces intermediate α-hydroxymethylNNAL (**6**) and then decomposes to 4-(3-pyridyl)-4-hydroxybutane-1-diazohydroxide (**9**), which reacts with DNA to form both pyridylhydroxybutyl (PHB) base adducts[11] and pyridylhydroxybutyl phosphate adducts [B_1p(PHB)B_2] (Figure

Received: October 10, 2017
Published: November 13, 2017

DOI: 10.1021/acs.chemrestox.7b00281
Chem. Res. Toxicol. 2018, 31, 48−57

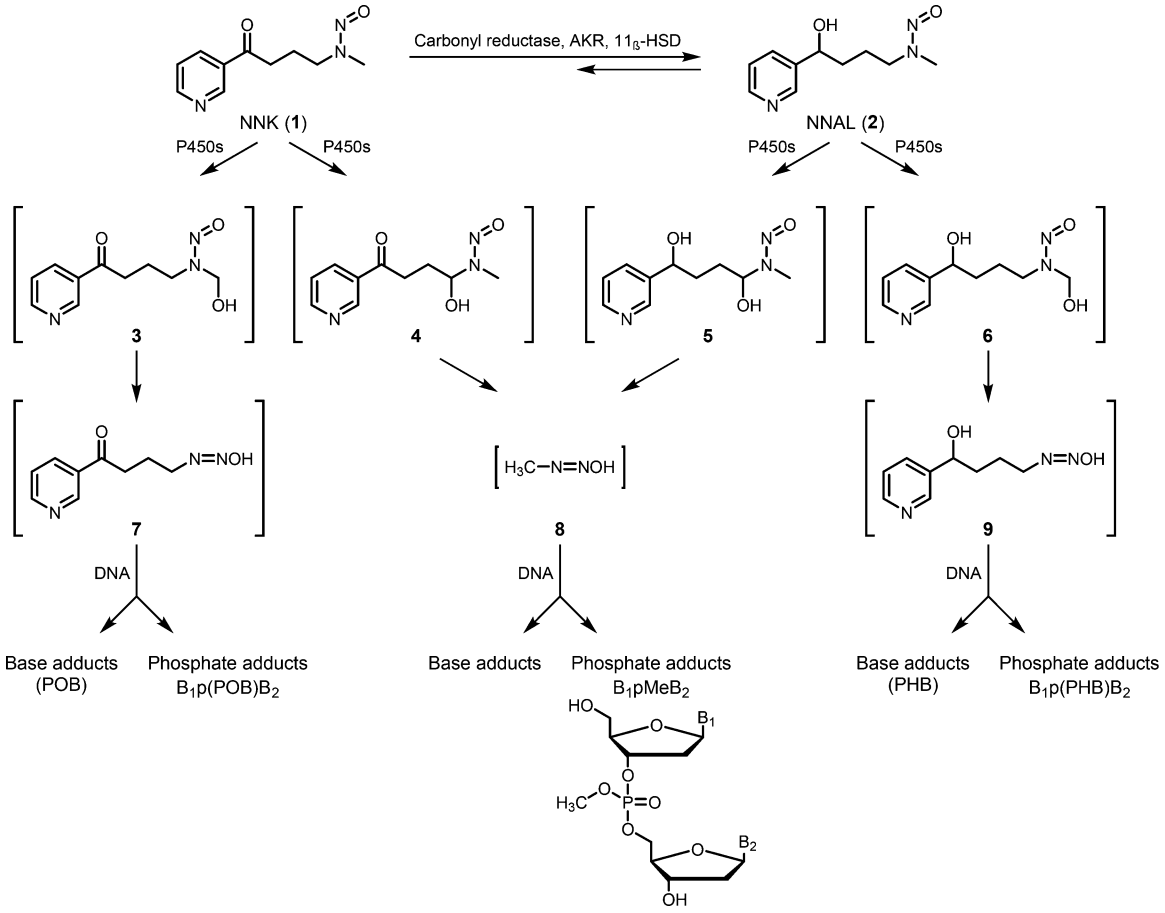

Figure 1. Formation of methyl DNA phosphate adducts by NNK and NNAL.

1).[12] The major POB and PHB base adducts and $B_1p(POB)B_2$ and $B_1p(PHB)B_2$ phosphate adducts have been characterized, and their levels in NNK- and NNAL-treated animals have been quantified in our laboratory.[4,8,10−14] α-Hydroxylation also occurs on the α-methylene carbons of NNK and NNAL, which produces intermediates α-methylenehydroxyNNK (**4**) and α-methylenehydroxyNNAL (**5**), respectively. Both **4** and **5** decompose to methane diazohydroxide (**8**), which reacts with DNA to form methyl DNA base adducts (Figure 1).[1] However, the formation of methyl DNA phosphate adducts and their levels in NNK- and NNAL-treated animals are still unknown.

The formation of methyl DNA phosphate adducts by other methylating agents has been reported previously.[15−24] The first identified methyl phosphate adduct, thymidylyl(3′-5′)thymidine methyl phosphotriester (TpMeT), was detected in rat liver DNA treated *in vitro* with the carcinogen *N*-methyl-*N*-nitrosourea (MNU).[16] Two other methyl phosphate adducts, TpMeA and TpMeC, together with TpMeT were detected in salmon sperm DNA treated with MNU or dimethyl sulfate (DMS).[18] TpMeT was also detected and quantified in salmon testis DNA and mouse lymphoma cells treated with MNU or methylmethanesulfonate (MMS).[19,20] The levels of methyl phosphate adducts were also measured *in vivo*. Following intraperitoneal treatment of male mice with MNU, DMS, or MMS, methyl phosphate adducts were detected, and their total amounts were measured in liver DNA.[21] The levels of methyl phosphate adducts were measured in tissue DNA of mice treated with MNU by single or multiple intraperitoneal injections.[22] In addition to the aforementioned direct-acting methylating agents, methyl DNA phosphate adducts were also formed by certain nitrosamines upon metabolic activation. For example, methyl phosphate adducts were detected in rats treated with *N*-nitrosodimethylamine (NDMA).[23,24] Based on these studies, NNK and NNAL also have the potential to form methyl DNA phosphate adducts, which is the focus of this study.

We developed a novel liquid chromatography (LC)-nanoelectrospray ionization (NSI)-high-resolution tandem mass spectrometry (HRMS/MS)-based method for analysis of methyl DNA phosphate adducts, referred to as B_1pMeB_2 adducts in this study. The B_1pMeB_2 adducts were characterized and quantified in lung DNA of rats treated with NNK, (*S*)-NNAL, or (*R*)-NNAL in the drinking water for 10, 30, 50, and 70 weeks.

EXPERIMENTAL PROCEDURES

Caution: *NNK, NNAL, and MNU are carcinogenic. They should be handled in a well-ventilated hood with extreme care and with personal protective equipment.*

Materials and Chemicals. TpMeT was purchased from MRIGlobal (Kansas City, MO), and its structure was confirmed by 1D and 2D NMR in our laboratory (Figure S1). MNU was obtained from Sigma-Aldrich Chemical Co. (Milwaukee, WI). $[^{13}C_{10}{}^{15}N_2]$TpT was prepared in another study.[12] Reagents and enzymes for DNA isolation were obtained from Qiagen Sciences (Germantown, MD). All other chemicals and solvents were purchased from Sigma-Aldrich Chemical Co. (Milwaukee, WI) or Fisher Scientific (Fairlawn, NJ).

Synthesis of $[^{13}C_{10}{}^{15}N_2]$TpMeT. $[^{13}C_{10}{}^{15}N_2]$TpMeT was synthesized by reacting $[^{13}C_{10}{}^{15}N_2]$TpT with MNU in 0.1 M Tris/EDTA buffer (pH 7.4) at 37 °C for 2.5 h and purified using a 30-mg Strata X cartridge (Phenomenex) activated with 2 mL of MeOH and 2 mL of H_2O. The cartridge was washed with 2 mL of H_2O and 1 mL of 10%

DOI: 10.1021/acs.chemrestox.7b00281
Chem. Res. Toxicol. 2018, 31, 48−57

MeOH sequentially and finally eluted with 2 mL of 50% MeOH. The presence of two diastereomers of [$^{13}C_{10}{}^{15}N_2$]TpMeT in the 50% MeOH fraction was confirmed by comparison with their corresponding unlabeled TpMeT standard (Figure S1) by using the LC-NSI-HRMS/MS method described below (Figure S2).

Rat Lung DNA Samples. The DNA samples were from male F-344 rats (n = 3 per group) in the control group and rats treated chronically with 5 ppm of NNK, (*S*)-NNAL, or (*R*)-NNAL in their drinking water for 10, 30, 50, and 70 weeks.[4] DNA was isolated using our previously developed protocol[8] and stored at −20 °C until analysis.

DNA Hydrolysis and Sample Preparation. The DNA samples were dissolved in 0.6 mL of 10 mM sodium succinate (pH 7.4) buffer containing 5 mM $CaCl_2$ and 5 fmol [$^{13}C_{10}{}^{15}N_2$]TpMeT as internal standard, followed by the addition of deoxyribonuclease I (0.75 units), phosphodiesterase I (0.005 units), and alkaline phosphatase (0.4 units). The solution was then incubated overnight at 37 °C. On the next day, 20 μL of hydrolysate was collected for dGuo analysis by HPLC-UV and DNA quantitation.[8] The remaining hydrolysate was filtered through 10 K centrifugal filters (Ultracel YM-10, Millipore), and the filtrates were loaded on 30 mg Strata X cartridges (Phenomenex) activated with 2 mL of MeOH and 2 mL of H_2O. The cartridges were washed with 2 mL of H_2O and 1 mL of 10% MeOH sequentially and finally eluted with 2 mL of 50% MeOH. The 50% MeOH fraction containing analytes was concentrated to dryness in a centrifugal evaporator. The residue was redissolved in 15 μL of deionized H_2O prior to analysis by LC-NSI-HRMS/MS.

LC-NSI-HRMS/MS Analysis. The analysis was performed on an Orbitrap Fusion Tribrid mass spectrometer (Thermo Scientific, Waltham, MA) with full scan, selected-ion monitoring (SIM) and product ion scan data acquisition using Orbitrap detection with internal calibration using the EASY-IC feature of the instrument. A nanoLC column (75 μm i.d., 360 μm o.d., 20 cm length, and 10 μm orifice) packed with Luna C_{18} bonded separation media (Phenomenex, Torrance, CA) was used. The mobile phase consisted of 2 mM NH_4OAc and CH_3CN. The sample (4 μL) was loaded onto the column with a 900 nL/min flow rate under the initial conditions for 6.5 min at which point the injection valve position was switched to take the injection loop out of the flow path, and the flow rate was reduced to 300 nL/min. Separation on the column was performed with increasing CH_3CN from 2−10% over 1.5 min and then from 10−15% over 28 min, followed by ramping to 90% CH_3CN within 2 min and holding at this composition for an additional 3 min. The gradient was then returned to 2% CH_3CN in 1 min, and the system was re-equilibrated at this mobile phase composition for 6 min at 900 nL/min before the next injection. The spray voltage of the mass spectrometer was 2.2 kV. The capillary temperature was 300 °C, and the S-Lens RF Level was 60%. A multiplexed selected-ion monitoring (SIM) analysis was performed whereby each ion mass of interest was sequentially isolated by the quadrupole and stored in the ion routing multipole, and upon collection of all masses of interest, all ions were transported into the Orbitrap for analysis. The $[M + H]^+$ ions of all possible phosphate adducts listed in Table 1 were analyzed in this fashion using an isolation window of 1.5 m/z, automatic gain control (AGC) target of 50,000, maximum inject time of 100 ms, and a resolution of 60,000. The product ion scan was performed using higher-energy collisional dissociation (HCD) fragmentation with a normalized collision energy of 20 units, isolation widths of 1.5 m/z for all the precursor ions, and product ion analysis performed with a mass range of m/z 100−700 at a resolution of 15,000. The accurate mass tolerance used for extraction of precursor and fragment ion signals was 5 ppm.

The quantitative analysis of TpMeT was performed using accurate mass extracted ion chromatograms of m/z 225.0870 $[C_{10}H_{13}N_2O_4]^+$ for TpMeT (parent ion m/z 561.2) and m/z 237.1146 for [$^{13}C_{10}{}^{15}N_2$]-TpMeT (parent ion m/z 573.2). Quantitation was based on the peak area ratio of TpMeT to [$^{13}C_{10}{}^{15}N_2$]TpMeT, the constructed calibration curves, and the amount of internal standard added. A calibration curve was constructed before each analysis using a series of standard solutions of TpMeT and [$^{13}C_{10}{}^{15}N_2$]TpMeT. The calibration standard solutions contained a constant amount of [$^{13}C_{10}{}^{15}N_2$]TpMeT (3 fmol on-column) and varying amounts of TpMeT (0.15, 0.3, 0.6, 1.5, 3, and 6 fmol on-column). The levels of other adducts were estimated on the basis of their MS signal intensities compared to TpMeT under SIM mode. All data are presented as mean ± standard deviation (SD). One-way ANOVA followed by a Bonferroni post test was used for multiple comparisons. A p value of <0.05 was considered significant.

Table 1. NNK and NNAL-Derived Methyl DNA Phosphate Adducts and Their $[M + H]^+$ Masses

			number of isomers detected		
B_1pMeB_2	$[M + H]^+$	possible	NNK	(*S*)-NNAL	(*R*)-NNAL
A-A	579.1824	2	2	2	2
C-C	531.1599	2	1	1	1
G-G	611.1722	2	2	2	2
T-T	561.1592	2	2	2	2
A-C	555.1711	4	4	3	3
A-G	595.1773	4	2	2	2
A-T	570.1708	4	3	3	3
C-G	571.1661	4	2	1	2
C-T	546.1596	4	2	2	2
G-T	586.1657	4	3	3	3
total		32	23	21	22

RESULTS

Characterization and Quantitation of Methyl Phosphate Adducts. Table 1 summarizes the possible numbers of methyl DNA phosphate adduct isomers which could be formed from intermediate **8** produced in the metabolism of NNK or NNAL. There can be 10 different combinations of the four nucleobases and different stereoisomers for each combination due to the tetrahedral structure of the phosphate group. Thus, there can be two possible isomers of B_1pMeB_2 with the same nucleobase combination and four isomers with different nucleobase combinations (two diastereomers of B_1-3′-pMe-5′-B_2 and two diastereomers of B_2-3′-pMe-5′-B_1), resulting in a total of 32 different possible B_1pMeB_2 adducts. By analyzing the data obtained from both SIM and product ion scans, as described below, we observed at least one isomer of each combination of B_1pMeB_2 phosphate adducts, and a total of 23, 21, and 22 out of 32 possible adducts were detected in the lung tissues of rats treated with NNK, (*S*)-NNAL and (*R*)-NNAL, respectively (Table 1).

Under our chromatographic conditions, the two diastereomers of TpMeT were observed upon analysis of the TpMeT standard (Figure 2A). The product ion spectra of the isomers showed similar fragmentation patterns, and only the spectrum of the isomer at 22.6 min with proposed fragmentation pathways is presented in Figure 2B. The identity of TpMeT was further confirmed by an MS^3 scan on the fragment ion m/z 337.0791, which was fragmented to two major ions m/z 225.0870 and m/z 207.0764 (Figure S1 and Figure 2B). The DNA samples from rat lung were analyzed using the same method. No TpMeT was detected upon analysis of DNA samples from control rats (Figure 3A), while both isomers of TpMeT were detected in rats treated with NNK (Figure 3B) or NNAL. The structures of all the other B_1pMeB_2 adducts were characterized based on the data obtained from LC-NSI-HRMS/MS analysis using SIM and product ion data acquisition of lung DNA samples of rats treated with NNK (Figure 4 and Figure S3). Taking ApMeC as an example, the exact mass of its precursor ion of m/z 555.1711 was monitored by SIM, and four peaks were detected (Figure 4), indicating the presence of four isomers. The fragmentation patterns of the two early eluting isomers were similar but with different abundances,

DOI: 10.1021/acs.chemrestox.7b00281
Chem. Res. Toxicol. 2018, 31, 48−57

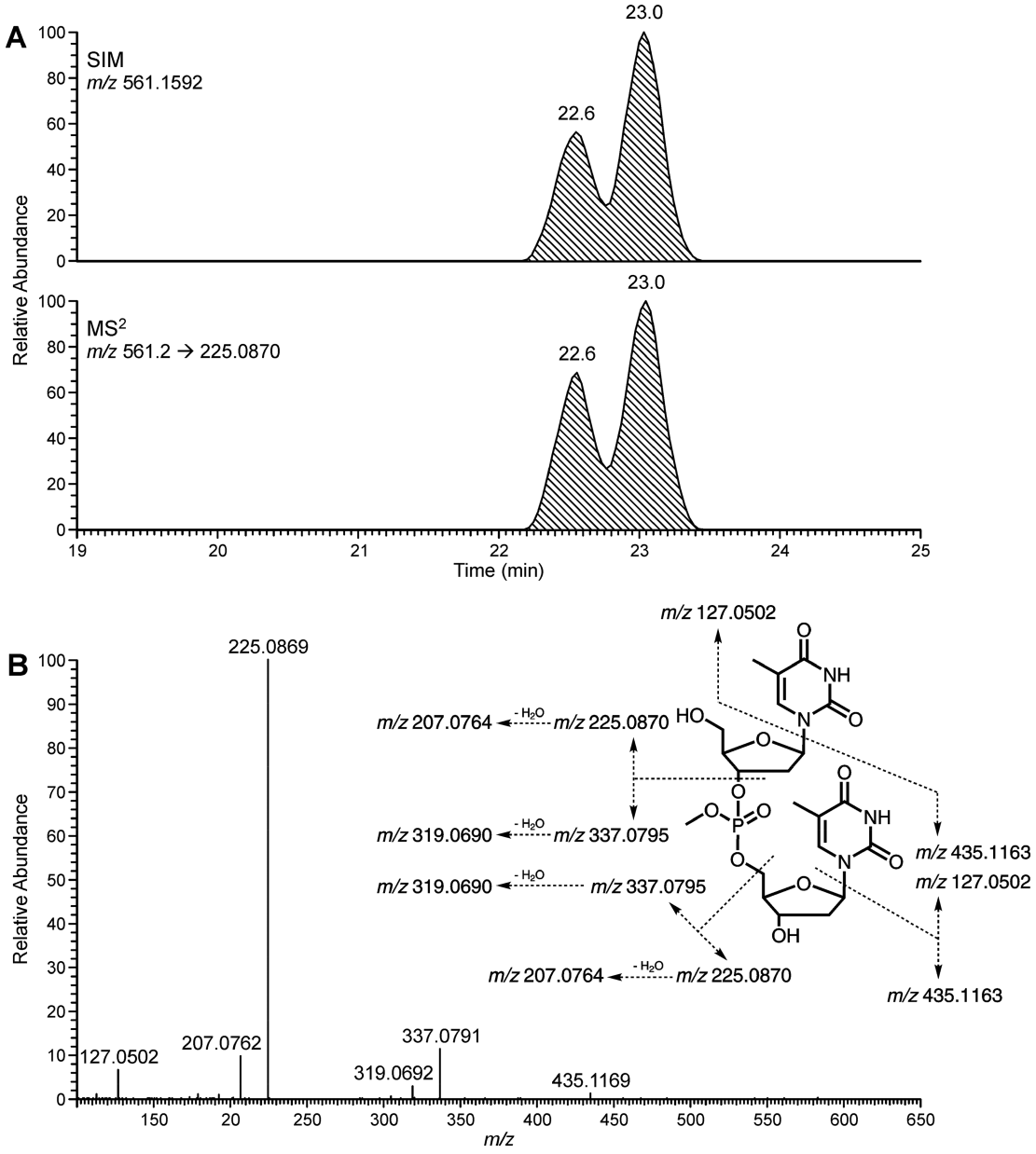

Figure 2. (A) The SIM of precursor ion (m/z 561.1592) and extracted fragment ion (m/z 561.2 → 225.0870) chromatograms obtained upon analysis of TpMeT standard (3 fmol on-column). (B) Product ion spectrum of one diastereomer (22.6 min) of TpMeT and its proposed fragmentation pathways.

and so were those of the two isomers which eluted later (Figure S4). However, the fragmentation patterns of the first two isomers were different compared to the latter two, which could be due to how the two sugar moieties of the nucleosides connect to the phosphorus atom, that is, A-3′-pMe-5′-C and C-3′-pMe-5′-A (Figure S4). The standards of ApMeC are currently unavailable, and further work needs to be done to assign the configuration of each isomer. The extracted ion chromatograms and fragmentation patterns for characterization of all the other B_1pMeB_2 phosphate adducts are available in Figure S3. None of the B_1pMeB_2 phosphate adducts were detected in control rats.

Using HCD fragmentation, several major fragment ions were generated in the product ion spectrum of TpMeT (Figure 2B). Because the highest signal intensities in the spectra of TpMeT and $[^{13}C_{10}{}^{15}N_2]$TpMeT were the transitions m/z 561.2 → 225.0870 and m/z 573.2 → 237.1146, respectively, they were selected for quantitative analysis. By using this method, a limit of detection of 0.15 fmol (on-column) was obtained for TpMeT. The instrument response and the TpMeT/$[^{13}C_{10}{}^{15}N_2]$TpMeT ratio were linear in the 0.15−6 fmol (on-column) range of TpMeT with a typical R^2 of 0.9982 (Figure 5).

Methyl Phosphate Adduct Levels in Rat Lung. In NNK-treated rats, the two major B_1pMeB_2 phosphate adducts with the highest levels in lung DNA were ApMeT and GpMeT, accounting for 38−54% and 16−20% of the total B_1pMeB_2 phosphate adducts, respectively (Figure 6A). For most of the B_1pMeB_2 adducts, the levels increased from 10 weeks of treatment to 30 weeks of treatment and persisted throughout the rest of the study. For example, the levels of ApMeT increased from 938 ± 124 fmol/mg DNA at 10 weeks of treatment to 1910 ± 95 fmol/mg DNA at 30 weeks of treatment ($p < 0.05$) and were not significantly changed afterward with levels of 1660 ± 172 and 1870 ± 73 fmol/mg DNA at 50 and 70 weeks, respectively.

DOI: 10.1021/acs.chemrestox.7b00281
Chem. Res. Toxicol. 2018, 31, 48−57

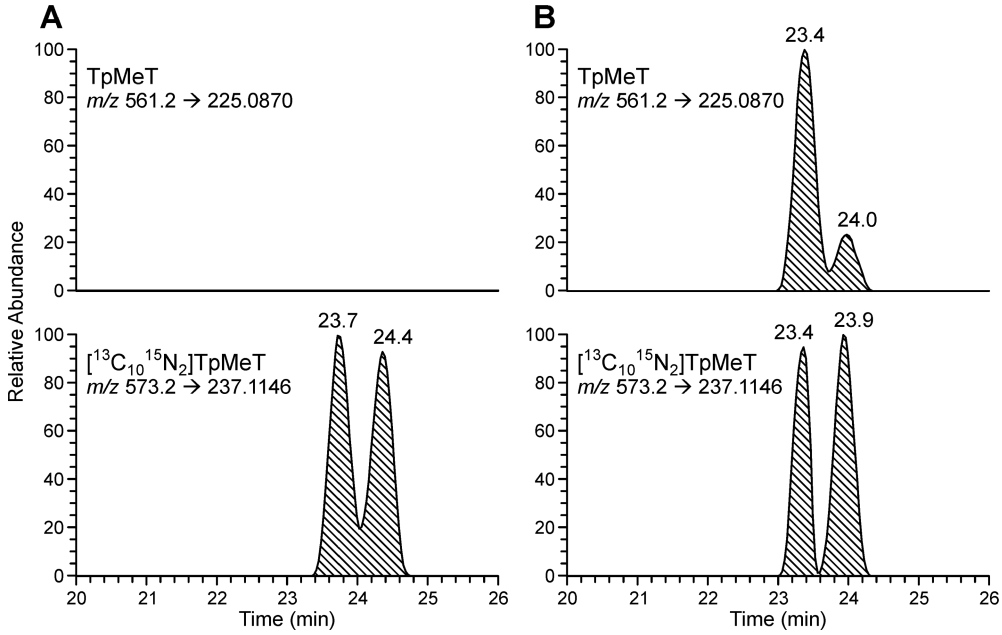

Figure 3. Typical chromatograms obtained upon analysis of TpMeT in rat lung DNA samples. (A) A control rat without NNK or NNAL treatment. (B) A rat treated chronically with 5 ppm of NNK in its drinking water for 30 weeks. No TpMeT was detected in the lung DNA from the control rat.

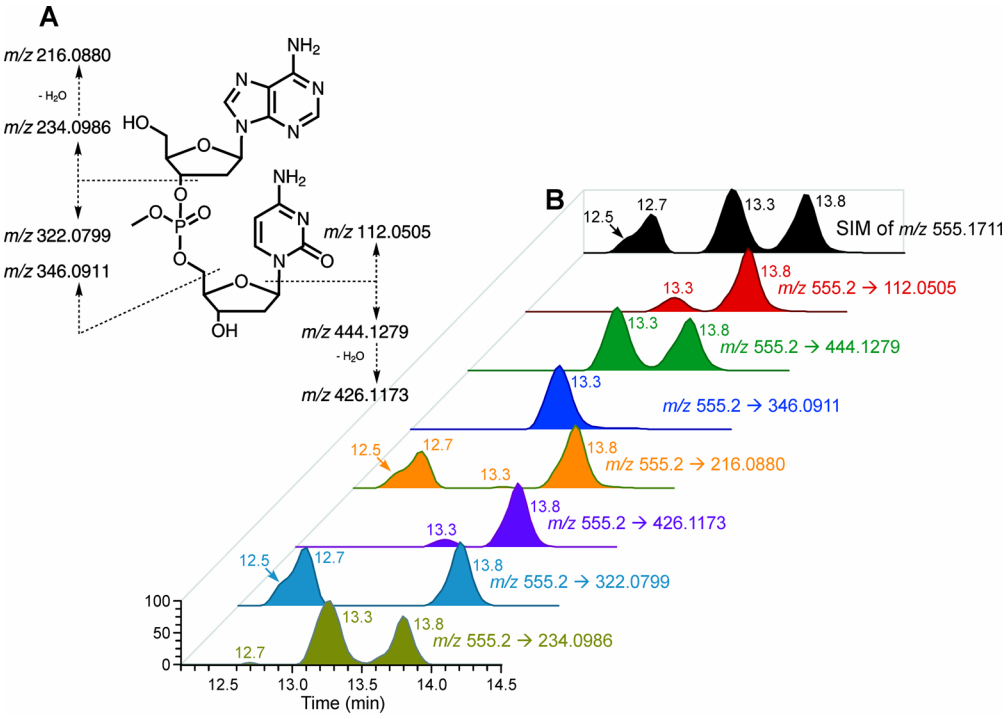

Figure 4. (A) Proposed fragmentation pattern and (B) the SIM of precursor ion and extracted fragment ion chromatograms of ApMeC in a lung DNA sample of a rat treated with NNK.

Similar to the NNK treatment group, the two major B_1pMeB_2 adducts in (*S*)-NNAL-treated rats were also ApMeT and GpMeT, which accounted for 37−55% and 13-21% of the total B_1pMeB_2 phosphate adducts, respectively (Figure 6B). The levels of most of the B_1pMeB_2 adducts did not significantly change over the course of the study. For example, the levels of GpMeT were 202 ± 48 fmol/mg DNA at 10 weeks of treatment and did not significantly change afterward with levels of 190 ± 60, 163 ± 57 and 170 ± 19 fmol/mg DNA at 30, 50, and 70 weeks, respectively.

In (*R*)-NNAL-treated rats, three major B_1pMeB_2 phosphate adducts were observed: ApMeT, GpMeT, and ApMeC, which accounted for 13−37%, 18−25%, and 13−23% of the total B_1pMeB_2 phosphate adducts, respectively (Figure 6C). For most of the B_1pMeB_2 adducts, the levels increased from 10 weeks of treatment to 30 weeks of treatment and decreased afterward. For example, the levels of ApMeC were 114 ± 22 fmol/mg DNA at 10 weeks of treatment reached a peak at 30 weeks (278 ± 14 fmol/mg DNA, $p < 0.05$) and decreased to 113 ± 15 fmol/mg DNA at 70 weeks of treatment.

DOI: 10.1021/acs.chemrestox.7b00281
Chem. Res. Toxicol. 2018, 31, 48−57

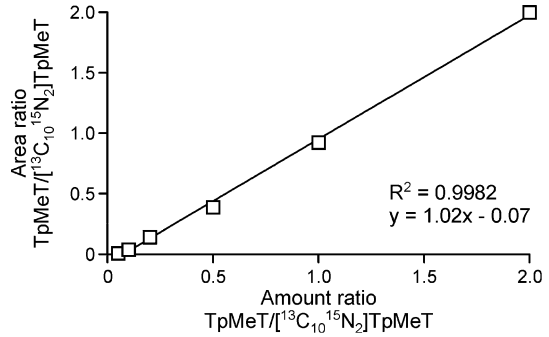

Figure 5. Linearity of TpMeT calibration curve. The amount of TpMeT in the calibration curve was increased from 0.15 fmol to 0.3, 0.6, 1.5, 3, and 6 fmol, with a constant amount of [$^{13}C_{10}{}^{15}N_2$]TpMeT (3 fmol).

Comparison of DNA Phosphate and Base Adducts. Six types of NNK-derived DNA adducts have been characterized so far: B_1pMeB_2 phosphate adducts, B_1p(POB)B_2 phosphate adducts, B_1p(PHB)B_2 phosphate adducts, methyl base adducts, POB base adducts, and PHB base adducts.[1,4,8,10,25] To determine the relative proportion of methyl phosphate adducts to the total measured DNA adducts formed in rats treated with NNK or NNAL, the levels of the other five types of adducts were obtained from our previous studies (Table 2).[4,10,12,13] The levels of total B_1p(POB)B_2 phosphate adducts in the lung of NNK-treated rats were reported previously.[10] The levels of total B_1p(POB)B_2 and B_1p(PHB)B_2 phosphate adducts in the lung of (*R*)- and (*S*)-NNAL-treated rats and total B_1p(PHB)B_2 phosphate adducts in the lung of NNK-treated rats were obtained from other studies.[12,13] The levels of one methyl base adduct, O^6-methylguanine, three major POB base adducts, O^2-[4-(3-pyridyl)-4-oxobut-1-yl]thymidine, 7-[4-(3-pyridyl)-4-oxobut-1-yl]guanine, and O^6-[4-(3-pyridyl)-4-oxobut-1-yl]-deoxyguanosine, and two major PHB base adducts, O^2-[4-(3-pyridyl)-4-hydroxybut-1-yl]thymidine and 7-[4-(3-pyridyl)-4-hydroxybut-1-yl]guanine, were reported previously.[4] Other NNK-derived methyl and POB base adducts have been previously identified from *in vitro* and *in vivo* studies,[1,9,26] but only the base adducts mentioned above were measured in the treated rats and included in this study.

Methyl phosphate adducts accounted for 15−38%, 8%, and 5−9% of the total measured DNA adducts in rats treated with NNK, (*S*)-NNAL, and (*R*)-NNAL, respectively (Figure 7). In the NNK-treated rats, methyl phosphate adducts accounted for 15% of the total adducts at 10 weeks of treatment, but became a major contributor afterward with 22%, 26%, and 38% of the total adducts at 30, 50, and 70 weeks, respectively. In the (*S*)-NNAL treatment group, B_1p(POB)B_2 phosphate adducts were the most abundant type at 10 weeks of treatment (34%), but decreased afterward (22%, 11%, and 10% at 30, 50, and 70 weeks of treatment, respectively). The other two abundant types of adducts were B_1p(PHB)B_2 phosphate adducts and POB base adducts, accounting for 27−32% and 23−39%, respectively, of the total measured DNA adducts. In the (*R*)-NNAL-treated rats, B_1p(PHB)B_2 phosphate adducts and PHB base adducts were the most abundant types of adducts, together accounting for 87−91% of the total measured DNA adducts. The total amount of measured DNA phosphate and base adducts were calculated and compared among the three treatment groups (Table 2). At 10 and 30 weeks of treatment, the total adduct levels in the NNK-treated rats were slightly higher than the other two treatment groups. At 50 weeks of treatment, the adduct levels were comparable between NNK and (*R*)-NNAL groups, which were higher than in the (*S*)-NNAL group ($p < 0.05$). There was no significant difference in the total adduct levels among the three groups at 70 weeks of treatment.

DISCUSSION

We investigated methyl DNA phosphate adduct formation by the tobacco-specific carcinogen NNK and enantiomers of its metabolite NNAL by using a novel, highly sensitive and specific LC-NSI-HRMS/MS method. A total of 23, 21, and 22 out of 32 possible methyl DNA phosphate adducts (B_1pMeB_2) were detected and quantified in the lung tissues of rats treated with NNK, (*S*)-NNAL, and (*R*)-NNAL, respectively. Taken together with our previous studies in which we characterized 30

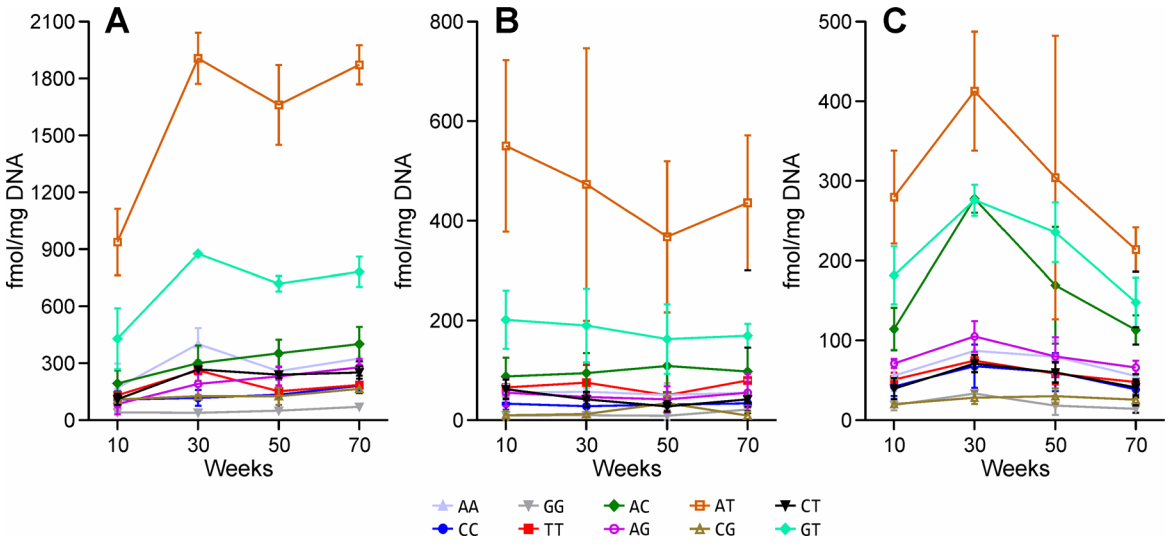

Figure 6. Levels of methyl DNA phosphate adducts in lung DNA of rats treated with 5 ppm of (A) NNK, (B) (*S*)-NNAL, and (C) (*R*)-NNAL in drinking water for 10, 30, 50, or 70 weeks. The levels of TpMeT were quantified based on the calibration curve and the amount of internal standard added in the samples, while the levels of other B_1pMeB_2 adducts were estimated on the basis of their MS signal intensities compared to TpMeT under SIM mode. Values are presented as means ± SD.

DOI: 10.1021/acs.chemrestox.7b00281
Chem. Res. Toxicol. 2018, 31, 48−57

Table 2. Levels of Total Methyl, $B_1p(POB)B_2$, $B_1p(PHB)B_2$ Phosphate Adducts, and Total Methyl, POB, PHB Base Adducts in Lung Tissue of Rats Treated with 5 ppm of NNK, (*S*)-NNAL, and (*R*)-NNAL in Drinking Water for 10, 30, 50, or 70 Weeks[a]

	DNA adduct (fmol/mg DNA)						
	phosphate adducts			base adducts[b]			
time (weeks)	B_1pMeB_2	$B_1p(POB)B_2$[c]	$B_1p(PHB)B_2$[d]	methyl	POB	PHB	total
			NNK				
10	2290 ± 546	475 ± 95	6390 ± 457	213 ± 27	4600 ± 440	1200 ± 49	15200 ± 844
30	4480 ± 119	417 ± 43	8160 ± 654	100 ± 65	5570 ± 195	1530 ± 104	20300 ± 705
50	3820 ± 215	346 ± 41	4000 ± 291	79 ± 15	5110 ± 327	1390 ± 74	14700 ± 495
70	4510 ± 129	218 ± 15	3950 ± 223	34 ± 48	2300 ± 473	869 ± 143	11900 ± 560
			(*S*)-NNAL				
10	1120 ± 217	4650 ± 356	3670 ± 67	269 ± 178	3180 ± 664	847 ± 34	13700 ± 807
30	1020 ± 290	2910 ± 109	4180 ± 119	114 ± 25	3950 ± 371	1210 ± 30	13400 ± 499
50	872 ± 309	1310 ± 77	3480 ± 79	78 ± 29	4530 ± 335	1250 ± 48	11500 ± 472
70	995 ± 258	1180 ± 204	3820 ± 582	49 ± 22	4470 ± 265	1270 ± 311	11800 ± 784
			(*R*)-NNAL				
10	874 ± 146	136 ± 32	4530 ± 368	5 ± 2	323 ± 36	4880 ± 721	10700 ± 824
30	1430 ± 140	135 ± 30	6670 ± 211	17 ± 23	490 ± 81	7440 ± 507	16200 ± 574
50	1100 ± 257	175 ± 17	6280 ± 336	7 ± 6	720 ± 46	6670 ± 885	15000 ± 982
70	763 ± 90	46[e]	6920 ± 436	4 ± 5	545 ± 112	6170 ± 1770	14400 ± 1830

[a]Values are presented as means ± SD (n = 3 or 5). [b]The data for base adduct levels are from Balbo, S. et al. (2014) *Carcinogenesis*, **35**, 2798−2806. [c]The data for $B_1p(POB)B_2$ phosphate adduct levels in NNK-treated rats are from Ma, B. et al. (2015) *Chem. Res. Toxicol.*, **28**, 2151−2159. [d]The data for $B_1p(PHB)B_2$ phosphate adduct levels in NNK-treated rats are from Ma, B. et al. (2017) *Carcinogenesis*, in press. The data for $B_1p(POB)B_2$ and $B_1p(PHB)B_2$ phosphate adduct levels in (*R*)-NNAL- or (*S*)-NNAL-treated rats are from Ma, B. et al. (2017) *Mutagenesis*, in press. [e]Single measurement.

$B_1p(POB)B_2$ adducts[10] and 107 $B_1p(PHB)B_2$ adducts,[12] we have collectively identified 160 different structurally unique DNA phosphate adducts in tissues of rats treated with NNK, which establishes NNK as the source of the most structurally diverse panel of DNA adducts identified to date from any carcinogen.

With a total of 32 possible methyl DNA phosphate adducts, the development of a suitable analytical method for simultaneous monitoring of all the possibilities is challenging, which could be one reason why the research on methyl phosphate adducts has still not been completely explored. Early attempts to detect methyl DNA phosphate adducts involved analysis of alkali-induced strand breaks at the sites of modified lesions. This method was based on the principle that addition of alkali should lead to the opening of imidazole ring of purines and block the spontaneous loss of methylated purines and leave the methyl DNA phosphate adducts as the only alkali-labile groups. Sedimentation coefficients of the hydrolyzed DNA samples were measured to determine the amount of methyl DNA phosphate adducts.[17,21,27,28] However, this method is not specific, and the levels may be overestimated if other alkali-labile lesions are present in the DNA. The ^{32}P-postlabeling technique, which was widely used for analysis of DNA base adducts, was another early effort applied to methyl phosphate adducts analysis. However, the traditional ^{32}P-postlabeling method for DNA base adduct analysis cannot be used for phosphate adducts because the negative charge on the phosphate group is neutralized by methylation.[29] In order to perform labeling, the methyl group had to be removed under alkaline conditions, and the resulting dinucleoside phosphates or 3′-phosphate alkylated mononucleotides were measured.[30,31] The analysis of methyl phosphate adducts was also conducted by a transalkylation approach, which utilized the weakly alkylating property of the methyl phosphate adducts for the transfer of the methyl group to strong nucleophiles, followed by measurement of methyl-nucleophile products.[32,33] All of the above-mentioned methods are indirect and unable to measure individual phosphate adducts. The first direct measurement of methyl phosphate adducts was analysis of TpMeT by mass spectrometry,[20] which was further optimized to achieve higher detection sensitivity.[19] Together with a method analyzing ethyl DNA phosphate adducts by mass spectrometry[34] and our successful characterization of $B_1p(POB)B_2$ phosphate adducts by an LC-NSI-HRMS/MS method,[10] the mass spectrometry-based approach has proved to be an appropriate technique for the analysis of methyl phosphate adducts. The method developed in this study is the first example of an HRMS/MS-based method being used for the analysis of methyl DNA phosphate adducts, demonstrating high sensitivity and selectivity for specific and accurate measurement of these adducts.

The formation patterns of methyl DNA phosphate and base adducts were different among the three treatment groups. In NNK-treated rats, the level of total methyl DNA phosphate adducts increased from 10 to 30 weeks of treatment and stayed constant afterward, while the methyl base adduct (O^6-methylguanine) levels decreased over the course of the study (Table 2). A decrease over time was observed for both methyl DNA phosphate and base adducts in (*S*)-NNAL-treated rats. In (*R*)-NNAL-treated rats, a decrease was also observed for methyl DNA phosphate adducts after 30 weeks of treatment, while the levels of O^6-methylguanine were low throughout the study. The greater persistence of methyl phosphate adducts compared to base adducts in NNK-treated rats was also observed in animals treated with other methylating agents. Following a single intraperitoneal injection of MNU to C57BL male mice at 80 mg/kg, the total methyl DNA phosphate adducts were measured in liver, lung, and kidney, and the half-life was estimated to be ∼7 days in all the three tissues. In contrast, the half-life of O^6-methylguanine was 13 h,[22] which was likely due to its repair by O^6-alkylguanine DNA alkyltransferase (AGT).[7] In another study, male Wistar rats were intraperitoneally injected with a single dose of NDMA at 10 mg/kg. TpMeT was detected and quantified in the liver with a half-life of 7 days, significantly longer than the

DOI: 10.1021/acs.chemrestox.7b00281
Chem. Res. Toxicol. 2018, 31, 48−57

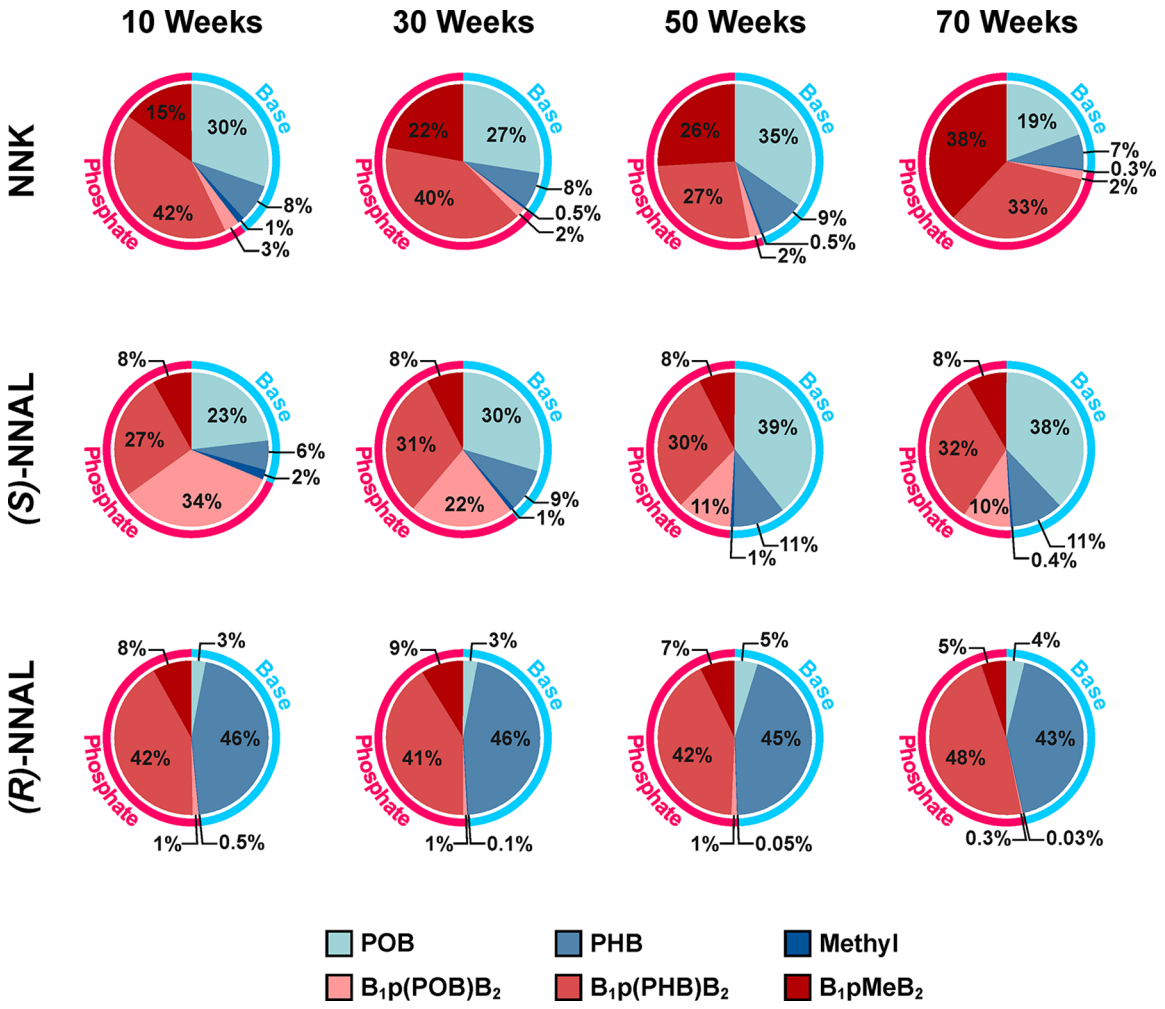

Figure 7. Relative levels of DNA phosphate and base adducts in lung DNA of rats treated with 5 ppm of NNK, (*S*)-NNAL, and (*R*)-NNAL in drinking water for 10, 30, 50, or 70 weeks. See the adduct levels in Table 2.

corresponding O^6-methylguanine with a half-life of 25 h.[24] The persistence of DNA phosphate adducts was also observed in our studies of pyridyloxobutyl[10] and pyridylhydroxybutyl[12,13] phosphate adducts in the NNK- and NNAL-treated rats. The persistence of these DNA phosphate adducts could be partially due to their chemical stability. TpMeT is stable at 37 °C for more than 3 days at pH 7.0 and has a half-life of 2.75 h even at pH 12.5.[35] However, depending on the type of alkyl group, not all the phosphate adducts are chemically stable. Tp(he)T, with the alkyl group being 2-hydroxyethyl moiety, has a half-life at 37 °C of only 60 min at pH 7.0 and <1 min at pH 12.5, possibly due to the formation of a reactive dioxaphospholane ring intermediate and subsequent rapid hydrolysis.[35] Another plausible explanation for the persistence of methyl DNA phosphate adducts is lack of repair mechanisms. The Ada protein in *E. coli* repairs methyl DNA phosphate adducts by transferring the aberrant methyl group to one of its own cysteine residues. However, this repair mechanism was only able to remove the (*S*)-stereoisomers of the methyl DNA phosphate adduct, while the (*R*)-stereoisomer was left unrepaired.[36,37] An alkyltransferase that repairs methyl DNA phosphate adducts was also detected in the eukaryote *Aspergillus nidulans*.[38] However, repair mechanisms for these adducts in higher eukaryotic organisms have not been discovered.

Taking into account the persistence of methyl DNA phosphate adducts, their biological consequences may be significant. An inhibitory effect on RNA synthesis by methyl DNA phosphate adducts was demonstrated *in vitro* by inhibiting exogenously added RNA polymerases, which occurred primarily at the initiation step.[39] Formation of methyl DNA phosphate adducts also neutralizes the negative charge of the internucleoside phosphodiester moiety, which affects the binding affinity of DNA to other macromolecules. A single charge difference due to methylation was shown to induce ~100-fold affinity difference of protein−DNA interactions.[40] Studies on other DNA phosphate adducts—ethyl and isopropyl—also showed their effects on DNA polymerases and DNA chain elongation.[41−43] However, the overall biological significance of DNA phosphate adducts, including methyl DNA phosphate adducts, remains largely unknown and warrants further investigation.

In contrast to structurally unique $B_1p(POB)B_2$ and $B_1p(PHB)B_2$ DNA phosphate adducts, which are specific to NNK and NNAL and possibly *N*′-nitrosonornicotine, methyl DNA phosphate adducts are also formed by other chemical methylating agents: MNU, DMS, MMS, and NDMA.[16,18,19,23] Thus, these adducts could also be potential biomarkers for exposure to these chemicals or could contribute to mechanistic understanding. For example, NDMA, which is classified as a Group 2A carcinogen (probably carcinogenic to humans) by the International Agency for Research on Cancer,[44] is widely detected in drinking water, foodstuffs, and alcoholic bever-

DOI: 10.1021/acs.chemrestox.7b00281
Chem. Res. Toxicol. 2018, 31, 48−57

ages.[45−47] The possible formation of methyl DNA phosphate adducts due to long-term exposure to NDMA or other DNA methylating agents could provide useful information on risk assessment in humans. In addition to environmental exposure, methylating agents are also used clinically for cancer treatment. Temozolomide, a prodrug for the treatment of glioblastoma multiforme, acts as a DNA methylating agent and forms O^6-methylguanine—the primary cytotoxic lesion—to exert its chemotherapeutic effects.[48] Formation of methyl DNA phosphate adducts by temozolomide and its potential clinical effects have not been studied, and such investigations could be conducted to provide more in-depth information.

CONCLUSION

We developed and applied a novel LC-NSI-HRMS/MS method to characterize and quantify methyl DNA phosphate adducts in the lungs of rats chronically treated with NNK, (*S*)-NNAL, or (*R*)-NNAL. A total of 23, 21, and 22 out of 32 possible adducts were detected in the three treatment groups, respectively. Certain methyl DNA phosphate adducts demonstrated persistence over the 70 weeks of treatment. These adducts could serve as potential biomarkers of chronic exposure to NNK and NNAL due to tobacco use and could also be used to study exposure to other chemical methylating agents.

ASSOCIATED CONTENT

Supporting Information

The Supporting Information is available free of charge on the ACS Publications website at DOI: 10.1021/acs.chemrestox.7b00281.

NMR and MS^3 data of TpMeT, chromatograms of TpMeT and [$^{13}C_{10}{}^{15}N_2$]TpMeT, chromatograms of B_1pMeB_2 phosphate adducts in rat lung DNA, product ion spectra and fragmentation pattern of ApMeC (PDF)

AUTHOR INFORMATION

Corresponding Author

*E-mail: bma@umn.edu. Tel: (612) 625-4925. Fax: (612) 624-3869.

ORCID

Irina Stepanov: 0000-0001-5140-8944

Stephen S. Hecht: 0000-0001-7228-1356

Funding

This study was supported by National Cancer Institute (NCI) grant CA-81301. Mass spectrometry analyses were carried out in the Analytical Biochemistry Shared Resource of the Masonic Cancer Center, supported in part by NCI grant CA-77598. Salary support for P.W.V. was provided by NCI grant CA-211256.

Notes

The authors declare no competing financial interest.

ACKNOWLEDGMENTS

We thank Xun Ming and Yingchun Zhao for their help with the mass spectrometry analysis and Bob Carlson for editorial assistance.

ABBREVIATIONS

DMS, dimethyl sulfate; HCD, higher-energy collisional dissociation; LC-NSI-HRMS/MS, liquid chromatography-nanoelectrospray ionization-high-resolution tandem mass spectrometry; MMS, methylmethanesulfonate; MNU, *N*-methyl-*N*-nitrosourea; NDMA, *N*-nitrosodimethylamine; NNK, 4-(methylnitrosamino)-1-(3-pyridyl)-1-butanone; PHB, pyridylhydroxybutyl; POB, pyridyloxobutyl; SD, standard deviation; SIM, selected-ion monitoring; TpMeT, thymidylyl(3′-5′)-thymidine methyl phosphotriester

REFERENCES

(1) Hecht, S. S. (1998) Biochemistry, biology, and carcinogenicity of tobacco-specific N-nitrosamines. *Chem. Res. Toxicol. 11*, 559−603.

(2) International Agency for Research on Cancer. (2012) Personal habits and indoor combustions. In *IARC Monographs on the Evaluation of Carcinogenic Risks to Humans*, v. 100E, pp 319−331, IARC, Lyon, France.

(3) Hecht, S. S., Stepanov, I., and Carmella, S. G. (2016) Exposure and metabolic activation biomarkers of carcinogenic tobacco-specific nitrosamines. *Acc. Chem. Res. 49*, 106−114.

(4) Balbo, S., Johnson, C. S., Kovi, R. C., James-Yi, S. A., O'Sullivan, M. G., Wang, M., Le, C. T., Khariwala, S. S., Upadhyaya, P., and Hecht, S. S. (2014) Carcinogenicity and DNA adduct formation of 4-(methylnitrosamino)-1-(3-pyridyl)-1-butanone and enantiomers of its metabolite 4-(methylnitrosamino)-1-(3-pyridyl)-1-butanol in F-344 rats. *Carcinogenesis 35*, 2798−2806.

(5) Ronai, Z. A., Gradia, S., Peterson, L. A., and Hecht, S. S. (1993) G to A transitions and G to T transversions in codon 12 of the Ki-ras oncogene isolated from mouse lung tumors induced by 4-(methylnitrosamino)-1-(3-pyridyl)-1-butanone (NNK) and related DNA methylating and pyridyloxobutylating agents. *Carcinogenesis 14*, 2419−2422.

(6) Jasti, V. P., Spratt, T. E., and Basu, A. K. (2011) Tobacco-specific nitrosamine-derived O^2-alkylthymidines are potent mutagenic lesions in SOS-induced Escherichia coli. *Chem. Res. Toxicol. 24*, 1833−1835.

(7) Peterson, L. A. (2017) Context matters: Contribution of specific DNA adducts to the genotoxic properties of the tobacco-specific nitrosamine NNK. *Chem. Res. Toxicol. 30*, 420−433.

(8) Lao, Y., Villalta, P. W., Sturla, S. J., Wang, M., and Hecht, S. S. (2006) Quantitation of pyridyloxobutyl DNA adducts of tobacco-specific nitrosamines in rat tissue DNA by high-performance liquid chromatography-electrospray ionization-tandem mass spectrometry. *Chem. Res. Toxicol. 19*, 674−682.

(9) Leng, J., and Wang, Y. (2017) Liquid chromatography-tandem mass spectrometry for the quantification of tobacco-specific nitrosamine-induced DNA adducts in mammalian cells. *Anal. Chem. 89*, 9124−9130.

(10) Ma, B., Villalta, P. W., Zarth, A. T., Kotandeniya, D., Upadhyaya, P., Stepanov, I., and Hecht, S. S. (2015) Comprehensive high-resolution mass spectrometric analysis of DNA phosphate adducts formed by the tobacco-specific lung carcinogen 4-(methylnitrosamino)-1-(3-pyridyl)-1-butanone. *Chem. Res. Toxicol. 28*, 2151−2159.

(11) Upadhyaya, P., Kalscheuer, S., Hochalter, J. B., Villalta, P. W., and Hecht, S. S. (2008) Quantitation of pyridylhydroxybutyl-DNA adducts in liver and lung of F-344 rats treated with 4-(methylnitrosamino)-1-(3-pyridyl)-1-butanone and enantiomers of its metabolite 4-(methylnitrosamino)-1-(3-pyridyl)-1-butanol. *Chem. Res. Toxicol. 21*, 1468−1476.

(12) Ma, B., Zarth, A. T., Carlson, E. S., Villalta, P. W., Upadhyaya, P., Stepanov, I., and Hecht, S. S. (2017) Identification of more than one hundred structurally unique DNA-phosphate adducts formed during rat lung carcinogenesis by the tobacco-specific nitrosamine 4-(methylnitrosamino)-1-(3-pyridyl)-1-butanone. *Carcinogenesis*, DOI: 10.1093/carcin/bgx135.

(13) Ma, B., Zarth, A. T., Carlson, E. S., Villalta, P. W., Stepanov, I., and Hecht, S. S. (2017) Pyridylhydroxybutyl and pyridyloxobutyl DNA phosphate adduct formation in rats treated chronically with enantiomers of the tobacco-specific nitrosamine metabolite 4-(methylnitrosamino)-1-(3-pyridyl)-1-butanol. *Mutagenesis*, DOI: 10.1093/mutage/gex031.

(14) Zhang, S., Wang, M., Villalta, P. W., Lindgren, B. R., Upadhyaya, P., Lao, Y., and Hecht, S. S. (2009) Analysis of pyridyloxobutyl and pyridylhydroxybutyl DNA adducts in extrahepatic tissues of F344 rats treated chronically with 4-(methylnitrosamino)-1-(3-pyridyl)-1-buta-

DOI: 10.1021/acs.chemrestox.7b00281
Chem. Res. Toxicol. 2018, 31, 48−57

none and enantiomers of 4-(methylnitrosamino)-1-(3-pyridyl)-1-butanol. *Chem. Res. Toxicol. 22*, 926−936.
(15) Jones, G. D., Le Pla, R. C., and Farmer, P. B. (2010) Phosphotriester adducts (PTEs): DNA's overlooked lesion. *Mutagenesis 25*, 3−16.
(16) Swenson, D. H., Farmer, P. B., and Lawley, P. D. (1976) Identification of the methyl phosphotriester of thymidylyl (3′,5′)-thymidine as a product from reaction of DNA with the carcinogen N-methyl-N-nitrosourea. *Chem.-Biol. Interact. 15*, 91−100.
(17) Shooter, K. V. (1978) DNA phosphotriesters as indicators of cumulative carcinogen-induced damage. *Nature 274*, 612−614.
(18) Swenson, D. H., and Lawley, P. D. (1978) Alkylation of deoxyribonucleic acid by carcinogens dimethyl sulphate, ethyl methanesulphonate, N-ethyl-N-nitrosourea and N-methyl-N-nitrosourea. Relative reactivity of the phosphodiester site thymidylyl(3′-5′)thymidine. *Biochem. J. 171*, 575−587.
(19) Zhang, F., Bartels, M. J., Pottenger, L. H., Gollapudi, B. B., and Schisler, M. R. (2007) Quantitation of lower levels of the DNA adduct of thymidylyl(3′-5′)thymidine methyl phosphotriester by liquid chromatography/negative atmospheric pressure chemical ionization tandem mass spectrometry. *Rapid Commun. Mass Spectrom. 21*, 1043−1048.
(20) Zhang, F., Bartels, M. J., Pottenger, L. H., Gollapudi, B. B., and Schisler, M. R. (2005) Quantitation of DNA adduct of thymidylyl(3′-5′)thymidine methyl phosphotriester by liquid chromatography/negative electrospray tandem mass spectrometry. *Rapid Commun. Mass Spectrom. 19*, 2767−2772.
(21) Shooter, K. V., and Merrifield, R. K. (1976) An assay for phosphotriester formation in the reaction of alkylating agents with deoxyribosenucleic acid in vitro and in vivo. *Chem.-Biol. Interact. 13*, 223−236.
(22) Shooter, K. V., and Slade, T. A. (1977) The stability of methyl and ethyl phosphotriesters in DNA in vivo. *Chem.-Biol. Interact. 19*, 353−361.
(23) Shooter, K. V., Slade, T. A., and O'Connor, P. J. (1977) The formation and stability of methyl phosphotriesters in the DNA of rat tissues after treatment with the carcinogen N,N-dimethylnitrosamine. *Chem.-Biol. Interact. 19*, 363−367.
(24) Den Engelse, L., Menkveld, G. J., De Brij, R. J., and Tates, A. D. (1986) Formation and stability of alkylated pyrimidines and purines (including imidazole ring-opened 7-alkylguanine) and alkylphosphotriesters in liver DNA of adult rats treated with ethylnitrosourea or dimethylnitrosamine. *Carcinogenesis 7*, 393−403.
(25) Lao, Y., Yu, N., Kassie, F., Villalta, P. W., and Hecht, S. S. (2007) Formation and accumulation of pyridyloxobutyl DNA adducts in F344 rats chronically treated with 4-(methylnitrosamino)-1-(3-pyridyl)-1-butanone and enantiomers of its metabolite, 4-(methylnitrosamino)-1-(3-pyridyl)-1-butanol. *Chem. Res. Toxicol. 20*, 235−245.
(26) Michel, A. K., Zarth, A. T., Upadhyaya, P., and Hecht, S. S. (2017) Identification of 4-(3-pyridyl)-4-oxobutyl-2′-deoxycytidine adducts formed in the reaction of DNA with 4-(acetoxymethylnitrosamino)-1-(3-pyridyl)-1-butanone: A chemically activated form of tobacco-specific carcinogens. *ACS Omega 2*, 1180−1190.
(27) Snyder, R. D., and Regan, J. D. (1981) Quantitative estimation of the extent of alkylation of DNA following treatment of mammalian cells with non-radioactive alkylating agents. *Mutat. Res. Lett. 91*, 307−314.
(28) Shooter, K. V. (1976) The kinetics of the alkaline hydrolysis of phosphotriesters in DNA. *Chem.-Biol. Interact. 13*, 151−163.
(29) Weinfeld, M., and Livingston, D. C. (1986) Synthesis and properties of oligodeoxyribonucleotides containing an ethylated internucleotide phosphate. *Biochemistry 25*, 5083−5091.
(30) Saris, C. P., Damman, S. J., van den Ende, A. M., Westra, J. G., and den Engelse, L. (1995) A 32P-postlabelling assay for the detection of alkylphosphotriesters in DNA. *Carcinogenesis 16*, 1543−1548.
(31) Guichard, Y., Jones, G. D., and Farmer, P. B. (2000) Detection of DNA alkylphosphotriesters by 32P postlabeling: evidence for the nonrandom manifestation of phosphotriester lesions in vivo. *Cancer Res. 60*, 1276−1282.
(32) Haglund, J., Ehrenberg, L., and Tornqvist, M. (1997) Studies of transalkylation of phosphotriesters in DNA: reaction conditions and requirements on nucleophiles for determination of DNA adducts. *Chem.-Biol. Interact. 108*, 119−133.
(33) Haglund, J., Rafiq, A., Ehrenberg, L., Golding, B. T., and Tornqvist, M. (2000) Transalkylation of phosphotriesters using Cob(I)alamin: toward specific determination of DNA-phosphate adducts. *Chem. Res. Toxicol. 13*, 253−256.
(34) Haglund, J., Van Dongen, W., Lemiere, F., and Esmans, E. L. (2004) Analysis of DNA-phosphate adducts in vitro using miniaturized LC-ESI-MS/MS and column switching: Phosphotriesters and alkyl cobalamins. *J. Am. Soc. Mass Spectrom. 15*, 593−606.
(35) Conrad, J., Muller, N., and Eisenbrand, G. (1986) Studies on the stability of trialkyl phosphates and di-(2′deoxythymidine) phosphotriesters in alkaline and neutral solution. A model study for hydrolysis of phosphotriesters in DNA and on the influence of a beta hydroxyethyl ester group. *Chem.-Biol. Interact. 60*, 57−65.
(36) Weinfeld, M., Drake, A. F., Saunders, J. K., and Paterson, M. C. (1985) Stereospecific removal of methyl phosphotriesters from DNA by an Escherichia coli ada+ extract. *Nucleic Acids Res. 13*, 7067−7077.
(37) McCarthy, T. V., and Lindahl, T. (1985) Methyl phosphotriesters in alkylated DNA are repaired by the Ada regulatory protein of E. coli. *Nucleic Acids Res. 13*, 2683−2698.
(38) Baker, S. M., Margison, G. P., and Strike, P. (1992) Inducible alkyltransferase DNA repair proteins in the filamentous fungus Aspergillus nidulans. *Nucleic Acids Res. 20*, 645−651.
(39) Marushige, K., and Marushige, Y. (1983) Template properties of DNA alkylated with N-methyl-N-nitrosourea and N-ethyl-N-nitrosourea. *Chem.-Biol. Interact. 46*, 179−188.
(40) He, C., Hus, J. C., Sun, L. J., Zhou, P., Norman, D. P., Dotsch, V., Wei, H., Gross, J. D., Lane, W. S., Wagner, G., and Verdine, G. L. (2005) A methylation-dependent electrostatic switch controls DNA repair and transcriptional activation by E. coli ada. *Mol. Cell 20*, 117−129.
(41) Miller, P. S., Chandrasegaran, S., Dow, D. L., Pulford, S. M., and Kan, L. S. (1982) Synthesis and template properties of an ethyl phosphotriester modified decadeoxyribonucleotide. *Biochemistry 21*, 5468−5474.
(42) Tsujikawa, L., Weinfield, M., and Reha-Krantz, L. J. (2003) Differences in replication of a DNA template containing an ethyl phosphotriester by T4 DNA polymerase and *Escherichia coli* DNA polymerase I. *Nucleic Acids Res. 31*, 4965−4972.
(43) Yashiki, T., Yamana, K., Nunota, K., and Negishi, K. (1992) Sequence specific block of in vitro DNA synthesis with isopropyl phosphotriesters in template oligodeoxyribonucleotides. *Nucleic Acids Symp. Ser. 27*, 197−198.
(44) International Agency for Research on Cancer. (1987) *Overall evaluations of carcinogenicity: An updating of IARC monographs*, Suppl. 7, p 67, IARC, Lyon, France.
(45) Krasner, S. W., Mitch, W. A., McCurry, D. L., Hanigan, D., and Westerhoff, P. (2013) Formation, precursors, control, and occurrence of nitrosamines in drinking water: a review. *Water Res. 47*, 4433−4450.
(46) Dybing, E., O'Brien, J., Renwick, A. G., and Sanner, T. (2008) Risk assessment of dietary exposures to compounds that are genotoxic and carcinogenic–an overview. *Toxicol. Lett. 180*, 110−117.
(47) Pflaum, T., Hausler, T., Baumung, C., Ackermann, S., Kuballa, T., Rehm, J., and Lachenmeier, D. W. (2016) Carcinogenic compounds in alcoholic beverages: an update. *Arch. Toxicol. 90*, 2349−2367.
(48) Zhang, J., Stevens, M. F., and Bradshaw, T. D. (2012) Temozolomide: mechanisms of action, repair and resistance. *Curr. Mol. Pharmacol. 5*, 102−114.

DOI: 10.1021/acs.chemrestox.7b00281
Chem. Res. Toxicol. 2018, 31, 48−57